# Light-responsive self-assembly of semi-conducting nanoplatelets

**Yesica FLORES ARIAS**
Sorbonne Université
**Rémi PLAMONT**
University of Groningen
**He Huang**
University of Groningen
**Alexander Ryabchun**
University of Groningen
**Nathalie Katsonis**
University of Twente https://orcid.org/0000-0003-1054-6544
**Benoit fleury** ( benoit.fleury@sorbonne-universite.fr )
Sorbonne Université https://orcid.org/0000-0003-4723-5037

**Article**

**Keywords:** semiconducting nanoplatelets, self-assembly, azobenzene ligands

**Posted Date:** August 20th, 2020

**DOI:** https://doi.org/10.21203/rs.3.rs-61203/v1

# Abstract

CdSe nanoplatelets are a recently discovered class of colloidal semiconducting nanocrystals. Atomic control over their thickness allows achieving control over quantum size effects, and in particular, these platelets exhibit monochromatic light emission because of the confinement of photo-generated excitons only in their thickness. These nanoplatelets can self-organize into supra-particular polymers, depending on their environment, which means that their shape anisotropy can be expressed at the microscale. Here, the self-assembly of semiconducting nanoplatelets is controlled remotely by light, in a dynamic nanoparticulate system that integrates light-responsive molecular switches covalently. Azobenzene ligands were thus designed to (*i*) be grafted on the nanoplatelets (*ii*) ensure their colloidal stability in chloroform when confined on their surface in the *E*-configuration. Upon irradiation, the ligands isomerize into their *Z*-configuration, leading to a modification of the dipolar moment of the particles and to the formation of one-dimensional stacks. The self-assembly is reversible, as thermal relaxation of the ligands yields the initial dispersion back. This reversible hybrid system can be used in the design of responsive optical systems, as illustrated by photo-patterning experiments leading to controlled spatial resolution of the luminescence intensity in thin films.


# Introduction

Involving nanoparticles into dynamic supra-particular systems allows tuning or switching the peculiar physical or chemical properties of these nano-objects.[1,2,3,4,5] In order to control nanoparticulate self-assembly remotely, light is a stimulus of choice since it can provide both spatial and temporal control over nanoparticle self-assembly.[6,7] Further, polarized incident light can also control their handedness.[8] The light-driven assembly of numerous nanoparticles has been investigated to date, however limited to spherical nanoparticles and to nanorods.[9,10,11,12] In parallel, new anisotropic nanoparticles have been synthesized and characterised and in particular, CdSe semi-conducting nanoplatelets with rectangular shapes.[13,14,15] These semiconducting nanocrystals present quantum confinement in only one direction thanks to the control of their thickness during the synthesis, and the radiative recombination of their photo-generated excitons arises therefore at very specific wavelengths with very narrow width, good quantum yields and fast emission.[16,17,18] The orientation of the transition dipoles involved in these rectangular nanoplatelets provides polarized emission and anisotropic emission patterns despite their symmetrical crystallographic structure.[19,20,21,22,23] Here, we couple the reversible photo-isomerisation of artificial molecular switches with the shape anisotropy of nanoplatelets, in order to create a dynamic system of supra-particular polymers associated with switchable luminescence properties. Importantly, these systems have the potential to provide pure emission colours in specific positions.[24]

Assembling semi-conducting nanoplatelets to harness their special properties into collective optical properties is ongoing challenge for physics and chemistry.[25] Abécassis and coworkers have shown that upon anti-solvent precipitation or after solvent evaporation, these semi-conducting nanoplatelets form supra-particular ribbons by aggregating face to face, and they consequently emit polarized light.[26]

Similar to the formation of nanoplatelets stacks upon solvent evaporation, the addition of oleic acid to a stable colloidal dispersion of CdSe nanoplatelets allowed the formation of the same kind of threads made of up to a thousand particles and the length of these threads could be controlled by tuning the amount of added oleic acid in a kind of “living polymer”.[27] The assembly of the nanoplatelets in these cases is mainly governed by depletion interactions and the final structures reach a minimum of energy.[28]

Our strategy consists in coupling nanoplatelets with azobenzene moieties in order to make a light-responsive dynamic system. Indeed, the nanoplatelets assemble during the light-generated meta-stable *Z*-state of the azobenzene, enabling therefore the reversibility of the process upon thermal relaxation of the molecules. In addition, the possibility to focus light beams, allowed us to spatially control the position of assembling domains.

## Results And Discussion

# Synthesis and characterisation of the light-responsive nanoplatelets

We prepared carboxylate-passivated nanoplatelets by following reported procedures.[13] These initial nanoplatelets were then reacted with thiol-functionalized azobenzene molecules 3-(4-(phenyldiazenyl)phenoxy)propane-1-thiol (**1**) or 3-(4-((4-(*tert*-butyl)phenyl)diazenyl)phenoxy)propane-1-thiol (**2**) as schematized on Fig. 1.

Thiols form strong and irreversible bonds with the surface $Cd^{2+}$ ions of II-VI semiconducting nanoparticules in a X-type bonding manner.[29,30,31,32] Given that both top and bottom sides of CdSe nanoplatelets are (100) crystallographic planes, and terminated by Cd atoms,[33] the thiol ligands are likely attached to these planes.

The reactions between ligands (**1**) and (**2**) and native nanoplatelets were monitored by absorption spectroscopy (Fig. 2a). After this procedure, both absorption bands were significantly red-shifted, from $\lambda = 510$ nm and $\lambda = 479$ nm to respectively $\lambda = 515$ nm and $\lambda = 485$ nm. Such a red shift is typical for capping ligands such as aliphatic thiols coating CdSe nanoplatelets,[34] and thus indicates a successful ligand exchange procedure and that the nanoplatelets have not been damaged by oxidation during their functionalization. Indeed, oxygen can contribute to the formation of a CdO layer on the platelets surface, detectable by a blue shift of the UV-Vis absorption.[25] The typical red-shift observed by UV-visible spectroscopy after thiol functionalization is also observable by luminescence spectroscopy (Fig. 2b). Under excitation at $\lambda = 365$ nm, the nanoplatelets emission shifts from $\lambda = 514$ nm to $\lambda = 519$ nm for both samples. In addition, energy-dispersive X-ray spectroscopy (EDX) performed on Cd and S atoms during STEM imaging of nanoplatelets covered by ligand (**2**) reveals that 1/3 of surface Cd atoms are linked to a thiol, showing a good coverage of the nanoplatelets by this ligand (Supplementary Fig. 1).

# Light-induced and reversible self-assembly

TEM images of the nanoplatelets coated with (**1**) and dispersed in chloroform are shown Fig. 3a. The micrographs reveal both individual and self-assembled nanoplatelets. Individual platelets are homogeneously dispersed and lay flat on the TEM grid, while self-assembled platelets form short stacks of 4.6 nm in length and are made of up to ten platelets, with the platelets in the stacks oriented perpendicular to the substrate and interacting via π-π stacking between ligands. Upon exposure to UV light (λ = 365 nm, 1 min), the system is modified as the platelets self-assemble into long 1D-superstructures (Fig. 3b). The resulting supra-particular ribbons can be as long as 500 nm and typically involve hundreds of platelets stacked face-to-face. We interpret this result as follows: upon irradiation, the azobenzene ligands undergo *E-to-Z* isomerization that leads to an increase of dipolar moment, thus the interaction between ligands is enhanced and the self-assembly leads to the formation of supraparticular ribbons. The light-induced self-assembly of these nanoplatelets is consistent with the dynamic behaviour of azobenzene-decorated gold nanoparticles that aggregate under UV light,[10] with the shape anisotropy of the platelets encoding for the final geometry of the assembled entities.

Decorating the CdSe nanoplatelets with ligand (**2**) allows addressing the role of inter-particle interactions further, as the $^{t}Bu$ group in the *para-* position of the azo group induces steric hindrance that forbids π-π stacking between the ligand molecules. TEM images of nanoplatelets coated with ligand (**2**) are shown Fig. 3c in their initial state. In contrast to platelets covered with ligand (**1**), platelets covered with **2** are well separated, they lay flat on the TEM substrate and not even short aggregates were formed. Upon irradiation (λ = 365 nm, 1 min), the nanoplatelets assemble into one dimensional stacks that reach 1μ m in length and can be composed by up to typically 200 nanoplatelets. Individual particles were scarcely observed (Fig. 3d).

Further the dispersions in chloroform of the nanoplatelets decorated by ligands (**1**) and (**2**) were checked by dynamic light scattering (DLS) measurements, in order to rule out the possible stacking of the nanoplatelets upon solvent evaporation when preparing the TEM grid. The results are shown in supplementary Table 1. Initially, the average hydrodynamic diameter of the particles covered by ligand (**1**) in solution is 110 nm. This size is larger than the physical diameter of the platelets, indicating that the nanoplatelets already show a tendency to aggregate in solution, even before UV irradiation. After irradiation, the average size of the objects in solution increases significantly to 545 nm, thus confirming that irradiation triggers the formation of long supra-particular ribbons. After 5 min of relaxation in ambient conditions, the data indicates a partial return to equilibrium since the size decreases to 212 nm. We understand this partial reversibility considering that once the nanoplatelets are attracted to one another by dipolar interactions, they can be trapped in this position by inter-particles Van-der-Waals interactions of remaining surface oleates. Finally, it is worth noting that from this intermediate equilibrium, the stacks can still grow since a second irradiation leads to an average size of 616 nm. A similar behaviour was observed for the nanoplatelets coated with ligand (**2**), however the initial hydrodynamic diameter was smaller (26 nm), *i.e.* corresponding to the lateral dimensions of an individual nanoplatelet. We conclude that using $^{t}Bu$-functionalized ligands enables a better dispersion of the particles in chloroform by forbidding any non-specific attractive inter-particles interactions. After

illuminating the solution during 1 min under UV light, the size indicated by DLS increases drastically to 425 nm revealing the efficient aggregation of the particles. Moreover, the reversibility of the process is also more efficient than in the case of ligand (**1**) since after relaxation during 5 min, the size decreases to 58 nm only. At last, the repeatability of the aggregation is shown by one more irradiation of the solution that allows an increase of the size to 375 nm. These results confirm that the modification of π–π stacking interactions is at the core of the dynamic self-assembling properties of this hybrid system.

Azobenzene ligands were thus grafted on the CdSe nanoplatelets effectively by using thiol groups. Our study also reveals that the choice of the surface ligands of the nanoplatelets is key to ensure a good dispersion of the particles in solution. The use of ligand (**2**) instead of ligand (**1**) allowed dispersing the platelets effectively at equilibrium, as $^{t}Bu$-groups prevented inter-particle π–π stacking. After *E-to-Z* conversion of ligand (**2**), the absence of aggregation but rather the formation of long ordered 1-D stacks shows that top and bottom faces of the nanoplatelets are covered by this ligand and that the decoration of these specific faces enables to take advantage of the shape anisotropy of the particles in order to drive their assembly into objects of predictable shape as already demonstrated by Abécassis and co-workers.[27]

In order to prove that the assembly process is triggered by azobenzene ligand isomerization, it was possible to detect the spectral signatures in chloroform of ligand (**2**) anchored on nanoplatelets before and after irradiation at λ = 365 nm and to compare it to the spectra of a chloroform solution of the free ligand. Figure 4a shows the UV-visible spectrum of free ligand (**2**) with a band at λ = 351 nm characteristic of the *E*-form of the molecule (orange spectrum). After one-minute irradiation of the solution at λ = 365 nm, this band vanishes and another band at λ = 310 nm appears (light blue spectrum), which is characteristic of the *Z*-form of the ligand. The solution is then left to relax in the dark at room temperature and after 5 minutes, half of the *E*-form was recovered (spectra from dark blue to pale purple). This behaviour can still be monitored once the ligands are anchored on the nanoplatelets. Figure 4b shows a light blue spectrum recorded on a chloroform solution of the nanoplatelets covered with ligand (**2**) right after their preparation. After one minute of irradiation at λ = 365 nm, the absorbance at λ = 351 nm drastically drops (purple spectrum), showing the conversion of the ligand. The characteristic band at λ = 310 nm of the *Z*-form of the ligand is nonetheless not observable because of the absorption of the nanoplatelets. After 5 minutes relaxation in the dark, the absorbance at λ = 351 nm is partially recovered (green spectrum) in accordance with the behaviour of the free ligand in solution. After exposure to ambient light, the initial spectrum is fully recovered. These results are consistent with DLS and TEM observations, pointing that the *Z*-form of the switch is responsible for the longitudinal stacking of the nanoplatelets.

From combined DLS, TEM and UV-visible spectroscopy investigations, we conclude that interfacing nanoplatelets with molecular switches enables their stacking under illumination, reversibly. Indeed, the energy input brought by UV light on nanoplatelets decorated by ligand (**2**) enables the efficient switch of the azo moieties (Fig. 5). This switch causes a change in the dipolar moment of the nanoplatelets driving them to stacking in chloroform. Subsequently, the initial dipolar moment is retrieved upon thermal relaxation of the azobenzene ligands, favouring the re-dispersion of the platelets in this solvent.

# Towards responsive optical systems

Using light as a trigger for nanoplatelet self-assembly opens new opportunities to involve these objects in optically active and specifically patterned optical materials. Upon stacking, the number of free nanoparticles in solution decreases. We therefore assumed that local irradiation of a thin film would lead to a local depletion in free nanoparticles that would be sufficient to create a gradient and thus cause the displacement of non-irradiated particles towards the irradiated zones.

We therefore prepared a thin film of nanoplatelets decorated by ligand (**2**) and covered it with a lithography mask made of 200 µm-wide stripes. The fluorescence of that film was recorded after irradiation, at a wavelength in which the switches do not isomerize.

The experimental set-up is schematized on Figs. 6a-b. Under a microscope lens, a mask was laid on an 80 µm-thick cell containing a solution of nanoplatelets decorated by ligand (**2**) in chloroform. *E*-to-*Z* isomerization of ligand (**2**) was then achieved by irradiation through a band pass filter ranging from $\lambda_{isom.}$ = 350 nm to $\lambda_{isom.}$ = 380 nm. The mask was then removed and the luminescence of the nanoplatelets was excited using another band pass filter ranging from $\lambda_{exc.}$ = 450 nm to $\lambda_{exc.}$ = 490 nm. As a reference, the sample luminescence was recorded before irradiation and without any mask (Fig. 6c). This blank sample reveals a homogenous film of dispersed particles. After irradiation through the mask, the luminescence intensity was increased under the irradiated zones comparatively to the masked zones (Fig. 6d). Homogeneous luminescence is fully recovered after 280 s (Fig. 6e). This experiment can be adapted to different scales as depicted by the same experiment leading to similar results with another mask (Supplementary Fig. 2). The results can be interpreted as follows: the stacking of the particles under UV light causes a drop in free particles concentration that is immediately compensated by a displacement of non-irradiated particles towards illuminated zones of the sample. In turn, the azobenzene ligands isomerize when entering the illuminated areas and the particles form self-assemblies. Once irradiation is stopped, the free particles concentration drops under masked zones, leading to a decrease of the luminescence intensity, while the number of stacked nanoplatelets is increased in the irradiated zones, which is associated with a higher luminescence intensity.

In conclusion, we show that (*i*) decorating nanoparticles with molecular switches allows promoting diffusion along gradients of concentration effectively and (*ii*) nanoplatelets, with their special optical properties, can be involved in the design of responsive optical devices. Given the unique luminescence properties of CdSe nanoplatelets, photopatterning self-assembled nanoplatelets allows designing dynamic and monochromatic luminescent patterns. Finally, we note that CdSe nanoparticles can be prepared in the form of dots, rods, platelets, tetrapods,[35,36] and even chiral shapes. Extending the functionalization strategy presented here, in combination with the self-assembly of various topologies or combinations of topologies, could lead to unusual and complex assemblies with emerging optical properties.[37]

# Methods

# Synthesis of CdSe nanoplatelets

In a three neck-flask, 80 mg of cadmium myristate are dispersed in 15 mL of octadecene by sonication during 20 to 30 min and 12 mg of selenium powder are added to the suspension and sonication is maintained for 15 min. The mixture is then stirred and degassed under vacuum at 90 °C for 1 h. After that, the mixture is heated up to 250 °C. At ∼135 °C the reaction is placed under argon atmosphere. At ∼195 °C, the solution becomes yellow-orange, and 82 mg of cadmium acetate $Cd(OAc)_2$ are added. The reaction is kept between 250 °C and 260 °C for 10 min and the mixture is cooled down to room temperature. At 220 °C, 5 mL of oleic acid are injected. The nanoplatelets are eventually purified by three cycles of precipitation in ethanol, centrifugation and dispersion in chloroform.

# Synthesis of 3-(4-(phenyldiazenyl)phenoxy)propane-1-thiol (1)

Compound A: 4-(allyloxy)phenyl-2-phenyldiazene: In a dried three neck round bottom flask, 4-(phenyldiazenyl)phenol (1.58 g, 8 mmol, 1 eq.), 3-bromoprop-1ene (0.7 mL, 0.97 g, 8 mmol, 1 eq.) and potassium t-butoxide (1 g, 10.4 mmol, 1.3 eq.) were dissolved in 20 mL of dry THF. The reaction mixture was stirred at reflux for 16 hours after what it was cool down to room temperature. The solvent was evaporated under reduced pressure and the residue dissolved in 100 mL $CH_2Cl_2$. The organic phase was washed with distilled water (3 × 60 mL). The organic phase was dried over $MgSO_4$ and the solvent was evaporated under reduced pressure. The product was purified by flash chromatography on silica with ethyl acetate / heptane (1:9) as eluent. The product was collected as an orange solid, 1.525 g, yield 80%. $^1$H NMR (400 MHz, $CDCl_3$) δ = 4.62 (t, 2H, O-$CH_2$), 5.39 (m, 2H, =$CH_2$), 6.08 (m, 1H, =CH-), 7.04 (d, 2H, Ar-H), 7.50 (m, 3H, Ar-H), 7.91 ppm (m, 4H, Ar-H).

Compound B: 3-(4-phenyldiazenyl)phenoxy)propyl-ethanethioate: In a dried three neck round bottom flask, compound A (1 g, 4.2 mmol, 1 eq.) and AIBN (1.45 g, 8.8 mmol, 2.1 eq.) were dissolved in 20 mL of dry toluene. Thioacetic acid (0.63 mL, 0.67 g, 8.8 mmol, 2.1 eq.) was added dropwise to the mixture under stirring. The reaction mixture was stirred at reflux for 16 hours. The reaction was then cool down to room temperature and diluted with 60 mL of toluene. The organic phase was washed with saturated $NaHCO_3$ solution in water (60 mL) and distilled water (2 × 60 mL). The organic phase was dried over $MgSO_4$ and the solvent was evaporated under reduced pressure. The product was purified by flash chromatography on silica with ethyl acetate / heptane (1:9) as eluent. The product was collected as an orange solid, 1 g, yield 76%. $^1$H NMR (400 MHz, $CDCl_3$) δ = 2.12 (m, 2H, C-$CH_2$-C), 2.36 (s, 3H, -$COCH_3$), 3.09 (t, 2H, $CH_2$-S), 4.10 (t, 2H, O-$CH_2$), 7.01 (d, 2H, Ar-H), 7.50 (m, 3H, Ar-H), 7.88 ppm (m, 4H, Ar-H).

3-(4-(phenyldiazenyl)phenoxy)propane-1-thiol (**1**): Compound B (0.5 g, 1.6 mmol, 1 eq.) was dissolved in 40 mL of degassed MeOH under $N_2$ followed by 2 g (9 eq) of $K_2CO_3$. 2 mL of HCl (37%) (14 eq.) were added dropwise and the reaction mixture was refluxed for 3 h. The reaction was then cool down to room

temperature and the excess HCl was neutralized with a NaOH solution in water (1M). 100 mL of $CH_2Cl_2$ were added to the reaction mixture and the organic phase was washed with distilled water (2 × 100 mL). The organic phase was collected and dried over $MgSO_4$ and the solvent was evaporated under reduced pressure. The product was purified by flash chromatography on silica with ethyl acetate / heptane (1:15) as eluent. The product was collected as an orange solid, 0.260 g, yield 60%. $^1$H NMR (400 MHz, $CDCl_3$) 1.42 (t, 1H, -SH), 2.12 (m, 2H, C-$CH_2$-C), 2.76 (m, 2H, S-$CH_2$), 4.16 (t, 2H, O-$CH_2$), 7.02 (d, 2H, Ar-H), 7.50 (m, 3H, Ar-H), 7.92 ppm (m, 4H, Ar-H). $^{13}$C NMR (100 MHz, $CDCl_3$) 21.30 ($CH_2$-S), 33.34 (C-$CH_2$-C), 66.06 ($CH_2$-O), 114.81 ($C_{Ar}$), 122.68 ($C_{Ar}$), 124.87 ($C_{Ar}$), 129.14 ($C_{Ar}$), 130.49 ($C_{Ar}$), 147.15 ($C_{Ar}$-N), 152.85 ($C_{Ar}$-N), 161.41 ppm ($C_{Ar}$-O)

# Synthesis of 3-(4-((4-( *tert* -butyl)phenyl)diazenyl)phenoxy)propane-1-thiol (2)

Compound D: 3-(4-((4-(tert-butyl)phenyl)diazenyl)phenoxy)propyl ethanethioate: In a dried three neck round bottom flask, 4-(4'(-tert-butyl)phenyldiazenyl)phenol (1.1 g, 4.3 mmol, 1 eq.), 3-bromoprop-1ene (0.7 mL, 0.52 g, 4.3 mmol, 1 eq.) and potassium t-butoxide (0.54 g, 5.6 mmol, 1.3 eq.) were dissolved in 20 mL of dry THF. The reaction mixture was stirred at reflux for 16 hours after what it was cool down to room temperature. The solvent was evaporated under reduced pressure and the residue dissolved in 100 mL $CH_2Cl_2$. The organic phase was washed with distilled water (3 × 60 mL). The organic phase was dried over $MgSO_4$ and the solvent was evaporated under reduced pressure. The product was purified by flash chromatography on silica with ethyl acetate / heptane (1:9) as eluent. The product was collected as an orange solid, 0.74 g, yield 58%. $^1$H NMR (400 MHz, $CDCl_3$) δ = 1.38 (s, 9 H, $CH_3$), 4.62 (t, 2H, O-$CH_2$), 5.41 (m, 2H, =$CH_2$), 6.08 (m, 1H, =CH-), 7.03 (d, 2H, Ar-H), 7.53 (d, 2H, Ar-H), 7.83 (d, 2H, Ar-H), 7.91 ppm (d, 2H, Ar-H).

Compound E: 3-(4-((4-(tert-butyl)phenyl)diazenyl)phenoxy)propane-1-thiol: In a dried three neck round bottom flask, compound A (0.74 g, 2.5 mmol, 1 eq.) and AIBN (0.87 g, 5.3 mmol, 2.1 eq.) were dissolved in 10 mL of dry toluene. Thioacetic acid (0.38 mL, 0.40 g, 5.3 mmol, 2.1 eq.) was added dropwise to the mixture under stirring. The reaction mixture was stirred at reflux for 16 hours. The reaction was then cool down to room temperature and diluted with 30 mL of toluene. The organic phase was washed with saturated $NaHCO_3$ solution in water (30 mL) and distilled water (2 × 30 mL). The organic phase was dried over $MgSO_4$ and the solvent was evaporated under reduced pressure. The product was purified by flash chromatography on silica with ethyl acetate / heptane (1:20) as eluent. The product was collected as an orange solid, 0.64 g, yield 72%. $^1$H NMR (400 MHz, $CDCl_3$) δ = 1.37 (s, 9 H, $CH_3$), 2.11 (m, 2H, C-$CH_2$-C), 2.35 (s, 3H, -$COCH_3$), 3.08 (t, 2H, $CH_2$-S), 4.09 (t, 2H, O-$CH_2$), 6.99 (d, 2H, Ar-H), 7.52 (d, 2H, Ar-H), 7.82 (d, 2H, Ar-H), 7.90 ppm (d, 2H, Ar-H).

3-(4-(phenyldiazenyl)phenoxy)propane-1-thiol (**2**): Compound B (0.6 g, 1.7 mmol, 1 eq.) was dissolved in 45 mL of degassed MeOH under $N_2$ followed by 2.1 g (9 eq) of $K_2CO_3$. 2.7 mL of HCl (37%) (19 eq.) were added dropwise and the reaction mixture was refluxed for 3 h. The reaction was then cool down to room temperature and the excess HCl was neutralized with a NaOH solution in water (1M). 100 mL of $CH_2Cl_2$ were added to the reaction mixture and the organic phase was washed with distilled water (2 × 100 mL). The organic phase was collected and dried over $MgSO_4$ and the solvent was evaporated under reduced pressure. The product was purified by flash chromatography on silica with ethyl acetate / heptane (1:15) as eluent. The product was collected as an orange solid, 0.330 g, yield 62%. $^1$H NMR (400 MHz, $CDCl_3$): 1.38 (s, 9 H, $CH_3$), 1.42 (t, 1H, -SH), 2.12 (m, 2H, C-$CH_2$-C), 2.76 (m, 2H, S-$CH_2$), 4.16 (t, 2H, O-$CH_2$), 7.02 (d, 2H, Ar-H), 7.50 (m, 3H, Ar-H), 7.92 ppm (m, 4H, Ar-H). $^{13}$C NMR (100 MHz, $CDCl_3$): 21.35 ($CH_2$-S), 31.44 ($CH_3$), 33.40 ($C_{tBu}$), 35.10 (C-$CH_2$-C), 66.08 ($CH_2$-O), 114.81 ($C_{Ar}$), 122.40 ($C_{Ar}$), 124.72 ($C_{Ar}$), 126.09 ($C_{Ar}$), 147.33 ($C_{Ar}$-N), 150.83 ($C_{Ar}$-N), 154.03 ($C_{Ar}$-*t*Bu), 161.21 ppm ($C_{Ar}$-O)

# Decoration of the nanoplatelets by ligands (1) and (2)

In a degassed colloidal solution of CdSe nanoplatelets in chloroform with an absorbance adjusted to 1, 15 mg of (**1**) or (**2**) are added together with a few droplets of triethylamine. The solution is stirred at 70 °C for one hour then cooled down to room temperature. Unreacted ligands are removed by cycles of centrifugation and dispersion in chloroform until no traces of ligand could be detected in the supernatant (UV-visible).

## Declarations

# Data availability

The data sets generated during the current study are available from the corresponding authors on reasonable request.

# Competing interests

The authors declare no competing financial or non-financial interests.

# Author contributions

N.K. and B.F. conceived and supervised the project. Y.F.A. planned and implemented the synthetic and analytical experiments on native nanoplatelets and decorated nanoplatelets. H.H. and R.P. performed the synthesis of the azobenzene molecules and contributed to the synthetic and analytical experiments on decorated nanoplatelets. A.R. planned and implemented the fluorescence microscopy experiments on thin films.

# Acknowledgements

This work was supported by CONACYT through the doctoral grant awarded to Yesica Flores Arias, the ANR Grant HSP No. ANR-16-CE09-0014-01, the French-Dutch program Van Gogh, the Merit Award Eole from the French-Dutch network attributed to Yesica Flores Arias, and the Volkswagen Foundation (Integration of Molecular Components in Functional Macroscopic Systems, 93424). The authors would like to thank Dr. Tibor Kudernac from the University of Groningen for his constant supporting help and advices, enabling the deep improvement of this work.

# References

1. Li, S. *et al.* Single- and multi-component chiral supraparticles as modular enantioselective catalysts. *Nat. Commun.* 10, 4826 (2019).
2. Kotov, N. A. Self-assembly of inorganic nanoparticles: Ab ovo. *EPL Europhys. Lett.* 119, 66008 (2017).
3. Grzelczak, M., Liz-Marzán, L. M. & Klajn, R. Stimuli-responsive self-assembly of nanoparticles. *Chem. Soc. Rev.* 48, 1342–1361 (2019).
4. Chu, Z. *et al.* Supramolecular Control of Azobenzene Switching on Nanoparticles. *J. Am. Chem. Soc.* 141, 1949–1960 (2019).
5. Boles, M. A., Engel, M. & Talapin, D. V. Self-Assembly of Colloidal Nanocrystals: From Intricate Structures to Functional Materials. *Chem. Rev.* 116, 11220–11289 (2016).
6. Bian, T., Chu, Z. & Klajn, R. The Many Ways to Assemble Nanoparticles Using Light. *Adv. Mater.* 1905866 (2019) doi:10.1002/adma.201905866.
7. Orlova, T., Plamont, R., Depauw, A. & Katsonis, N. Dynamic Spirals of Nanoparticles in Light-Responsive Polygonal Fields. *Small* vol. 15 http://onlinelibrary.wiley.com/doi/abs/10.1002/smll.201902419 (2019).
8. Kim, J.-Y. *et al.* Assembly of Gold Nanoparticles into Chiral Superstructures Driven by Circularly Polarized Light. *J. Am. Chem. Soc.* 141, 11739–11744 (2019).
9. Zhang, L. *et al.* Light-Triggered Reversible Self-Assembly of Gold Nanoparticle Oligomers for Tunable SERS. *Langmuir* 31, 1164–1171 (2015).
10. Manna, D., Udayabhaskararao, T., Zhao, H. & Klajn, R. Orthogonal Light-Induced Self-Assembly of Nanoparticles using Differently Substituted Azobenzenes. *Angew. Chem. Int. Ed.* 54, 12394–12397 (2015).
11. Zhao, H. *et al.* Reversible trapping and reaction acceleration within dynamically self-assembling nanoflasks. *Nat. Nanotechnol.* 11, 82–88 (2016).
12. Klajn, R., Wesson, P. J., Bishop, K. J. M. & Grzybowski, B. A. Writing Self-Erasing Images using Metastable Nanoparticle “Inks”. *Angew. Chem. Int. Ed.* 48, 7035–7039 (2009).

13. Ithurria, S. & Dubertret, B. Quasi 2D Colloidal CdSe Platelets with Thicknesses Controlled at the Atomic Level. *J. Am. Chem. Soc.* 130, 16504–16505 (2008).
14. Li, Z. & Peng, X. Size/Shape-Controlled Synthesis of Colloidal CdSe Quantum Disks: Ligand and Temperature Effects. *J. Am. Chem. Soc.* 133, 6578–6586 (2011).
15. She, C. *et al.* Red, Yellow, Green, and Blue Amplified Spontaneous Emission and Lasing Using Colloidal CdSe Nanoplatelets. *ACS Nano* 9, 9475–9485 (2015).
16. Lhuillier, E. *et al.* Two-Dimensional Colloidal Metal Chalcogenides Semiconductors: Synthesis, Spectroscopy, and Applications. *Acc. Chem. Res.* 48, 22–30 (2015).
17. Dufour, M. *et al.* Halide Ligands To Release Strain in Cadmium Chalcogenide Nanoplatelets and Achieve High Brightness. *ACS Nano* 13, 5326–5334 (2019).
18. Kelestemur, Y. *et al.* Colloidal CdSe Quantum Wells with Graded Shell Composition for Low-Threshold Amplified Spontaneous Emission and Highly Efficient Electroluminescence. *ACS Nano* 13, 13899–13909 (2019).
19. Feng, F. *et al.* Probing the Fluorescence Dipoles of Single Cubic CdSe/CdS Nanoplatelets with Vertical or Horizontal Orientations. *ACS Photonics* 5, 1994–1999 (2018).
20. Feng, F. *et al.* Consequence of shape elongation on emission asymmetry for colloidal CdSe/CdS nanoplatelets. *Nano Res.* 11, 3593–3602 (2018).
21. Gao, Y., Weidman, M. C. & Tisdale, W. A. CdSe Nanoplatelet Films with Controlled Orientation of their Transition Dipole Moment. *Nano Lett.* 17, 3837–3843 (2017).
22. Antanovich, A., Prudnikau, A. & Artemyev, M. Anisotropy of Structure and Optical Properties of Self-Assembled and Oriented Colloidal CdSe Nanoplatelets. *Z. Für Phys. Chem.* 232, 1619–1630 (2018).
23. Brumberg, A. *et al.* Determination of the In-Plane Exciton Radius in 2D CdSe Nanoplatelets via Magneto-optical Spectroscopy. *ACS Nano* 13, 8589–8596 (2019).
24. Sun, H. & Buhro, W. E. Core–Shell Cadmium Telluride Quantum Platelets with Absorptions Spanning the Visible Spectrum. *ACS Nano* 13, 6982–6991 (2019).
25. Tessier, M. D. *et al.* Phonon Line Emission Revealed by Self-Assembly of Colloidal Nanoplatelets. *ACS Nano* 7, 3332–3340 (2013).
26. Abécassis, B., Tessier, M. D., Davidson, P. & Dubertret, B. Self-Assembly of CdSe Nanoplatelets into Giant Micrometer-Scale Needles Emitting Polarized Light. *Nano Lett.* 14, 710–715 (2014).
27. Jana, S., Davidson, P. & Abécassis, B. CdSe Nanoplatelets: Living Polymers. *Angew. Chem. Int. Ed.* 55, 9371–9374 (2016).
28. Abécassis Benjamin. Three-Dimensional Self Assembly of Semiconducting Colloidal Nanocrystals: From Fundamental Forces to Collective Optical Properties. *ChemPhysChem* 17, 618–631 (2015).
29. Eychmüller Alexander & Rogach Andrey L. Chemistry and photophysics of thiol-stabilized II-VI semiconductor nanocrystals. *Pure Appl. Chem.* 72, 179 (2000).
30. Yeltik, A. *et al.* Experimental Determination of the Absorption Cross-Section and Molar Extinction Coefficient of Colloidal CdSe Nanoplatelets. *J. Phys. Chem. C* 119, 26768–26775 (2015).

31. Fritzinger, B., Capek, R. K., Lambert, K., Martins, J. C. & Hens, Z. Utilizing Self-Exchange To Address the Binding of Carboxylic Acid Ligands to CdSe Quantum Dots. *J. Am. Chem. Soc.* 132, 10195–10201 (2010).
32. Sih, B. C. & Wolf, M. O. CdSe Nanorods Functionalized with Thiol-Anchored Oligothiophenes. *J. Phys. Chem. C* 111, 17184–17192 (2007).
33. Knauf, R. R., Lennox, J. C. & Dempsey, J. L. Quantifying Ligand Exchange Reactions at CdSe Nanocrystal Surfaces. *Chem. Mater.* 28, 4762–4770 (2016).
34. Antanovich, A. *et al.* A strain-induced exciton transition energy shift in CdSe nanoplatelets: the impact of an organic ligand shell. *Nanoscale* 9, 18042–18053 (2017).
35. Peng, X. *et al.* Shape control of CdSe nanocrystals. *Nature* 404, 59–61 (2000).
36. Peng, Z. A. & Peng, X. Nearly Monodisperse and Shape-Controlled CdSe Nanocrystals via Alternative Routes: Nucleation and Growth. *J. Am. Chem. Soc.* 124, 3343–3353 (2002).
37. Yan, J. *et al.* Self-Assembly of Chiral Nanoparticles into Semiconductor Helices with Tunable near-Infrared Optical Activity. *Chem. Mater.* 32, 476–488 (2020).

# Figures

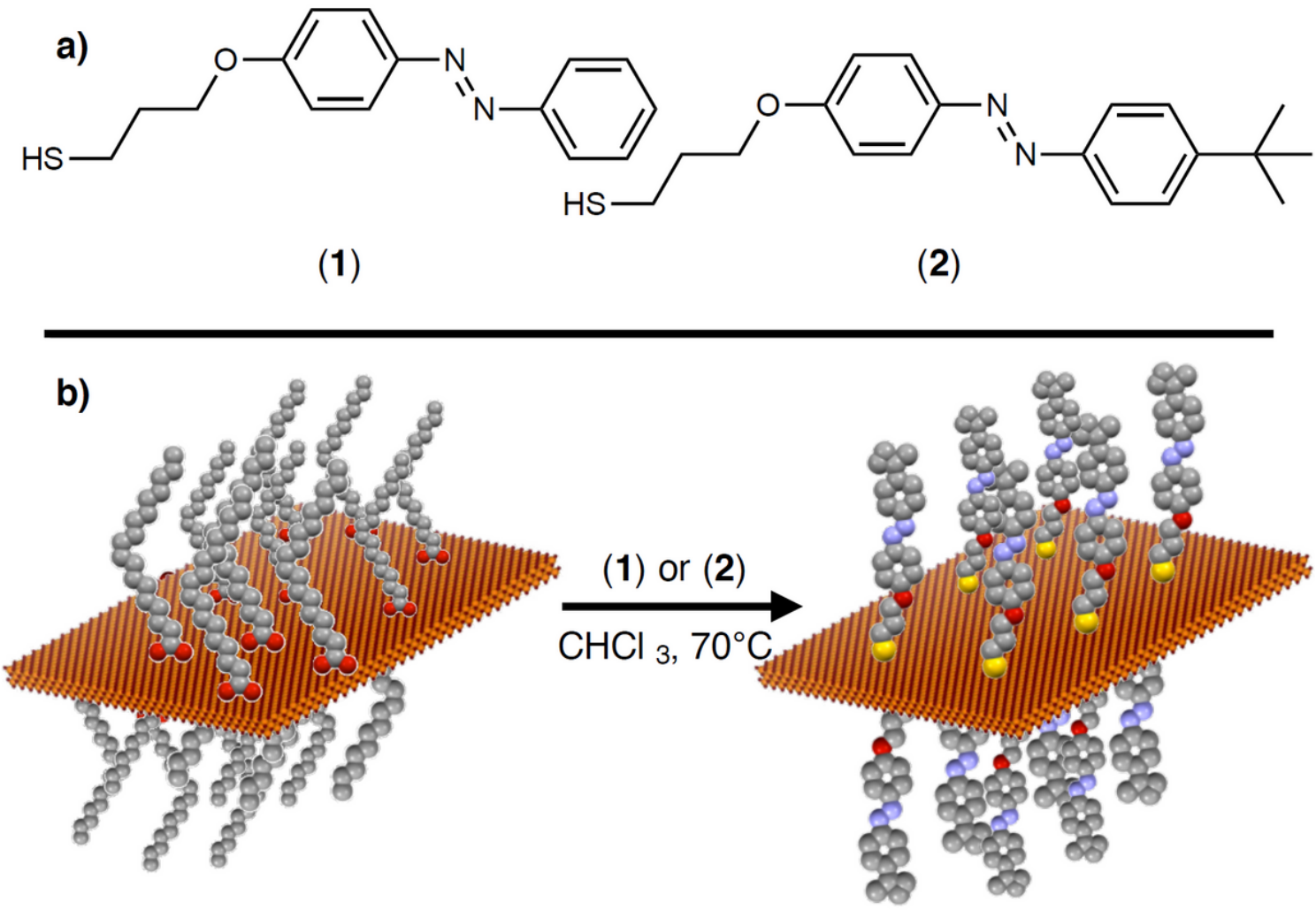


**Figure 1**

Decoration of CdSe nanoplatelets by thiol-functionalized azobenzene molecules. a) molecular formulas of ligands (1) and (2) used in this study. b) Schematic representation of the reaction at the surface of the nanoplatelets in order to exchange the native carboxylates by these ligands.

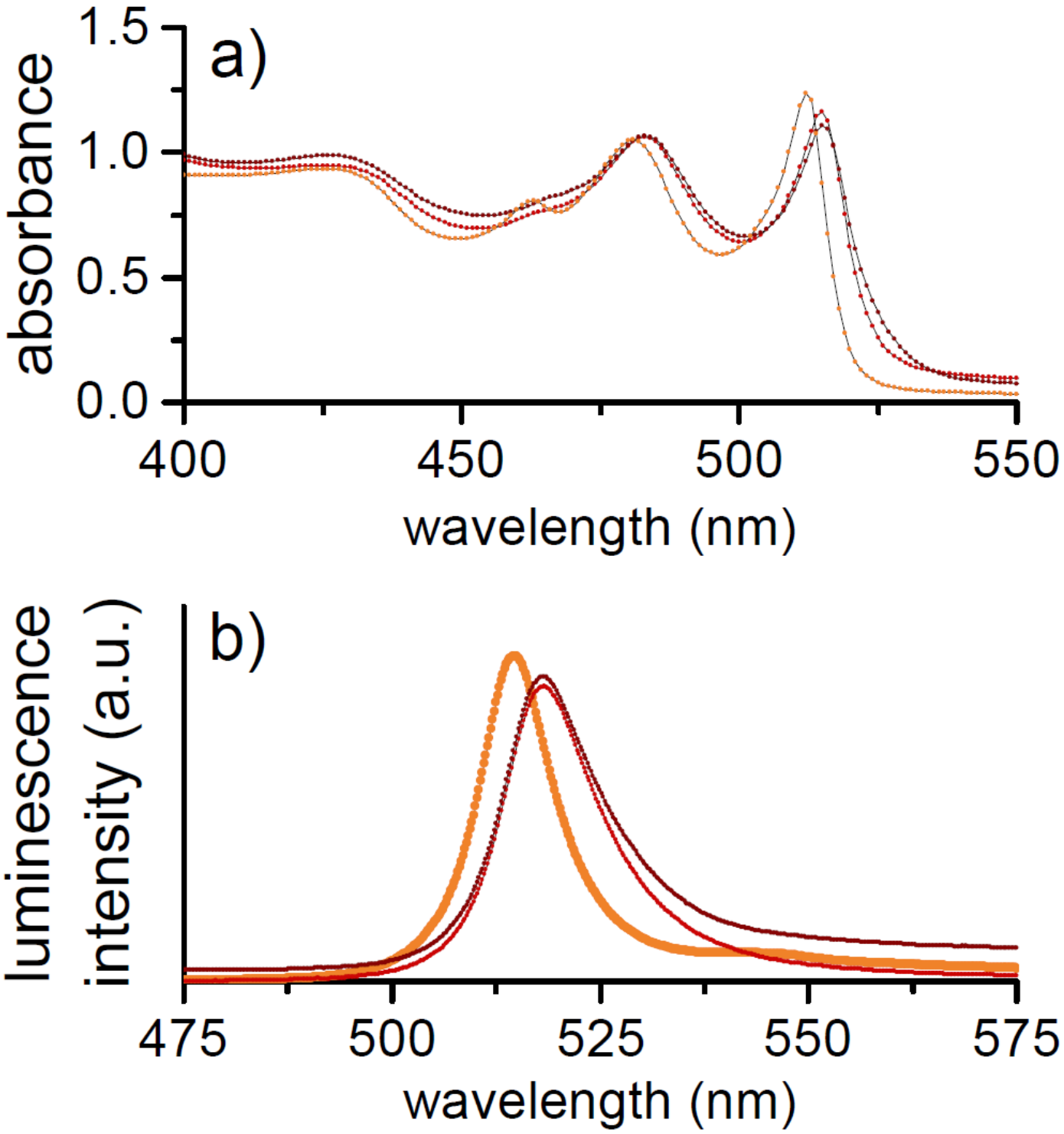


**Figure 2**

Comparison of the UV-visible and luminescence spectra of CdSe nanoplatelets before and after functionalization by ligands (1) and (2). a) UV-visible spectra of native (orange) CdSe nanoplatelets and CdSe nanoplatelets decorated by ligands (1) (dark red) and (2) (light red). b) luminescence spectra of native (orange) CdSe nanoplatelets and CdSe nanoplatelets decorated by ligands (1) (dark red) and (2) (light red).

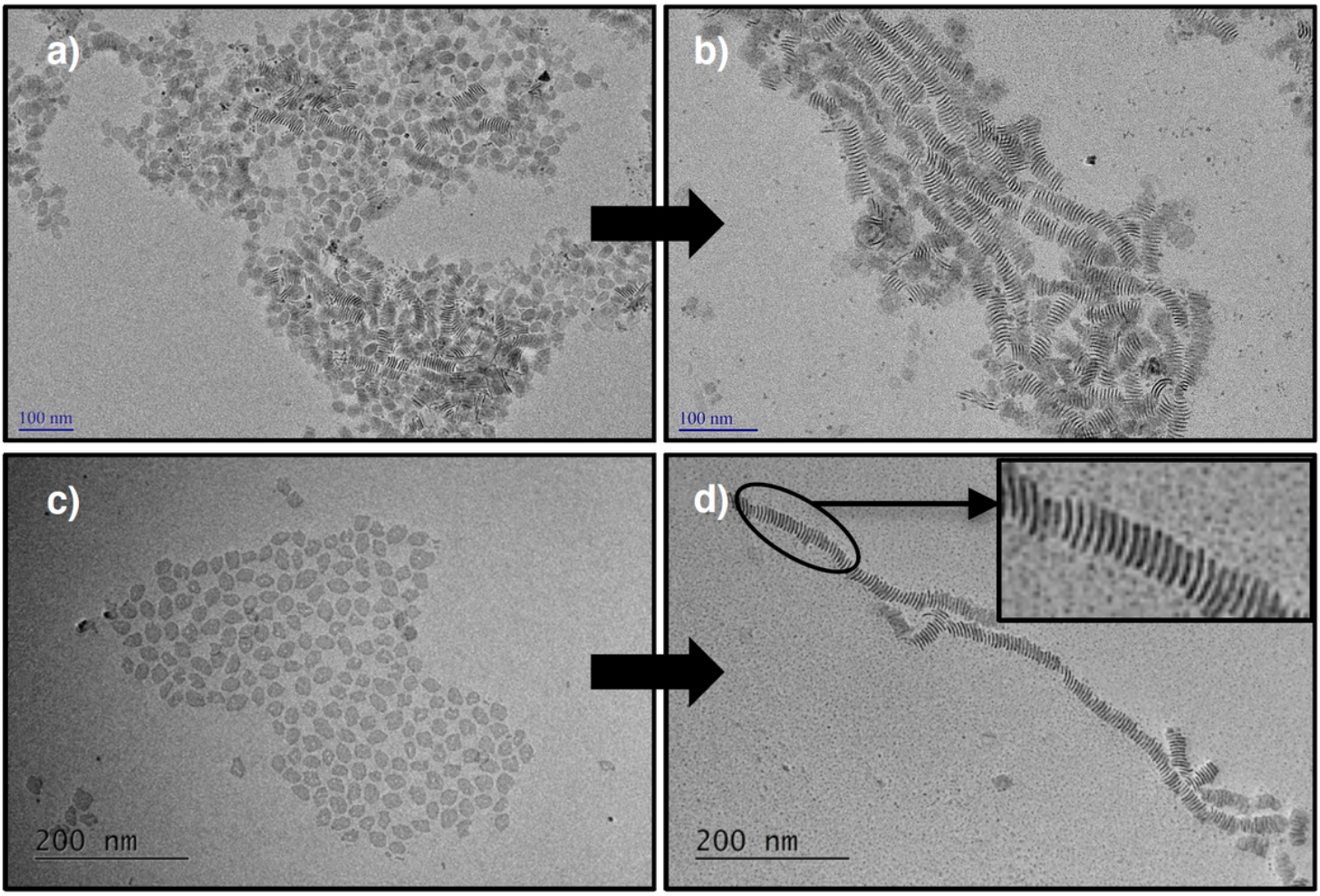


## Figure 3

TEM images of CdSe nanoplatelets. a) CdSe nanoplatelets decorated by ligand (1) before UV irradiation. b) CdSe nanoplatelets decorated by ligand (1) after UV irradiation. c) CdSe nanoplatelets decorated by ligand (2) before UV irradiation. d) CdSe nanoplatelets decorated by ligand (2) after UV irradiation. Scale bars are 100 nm (a, b) and 200 nm (c, d).

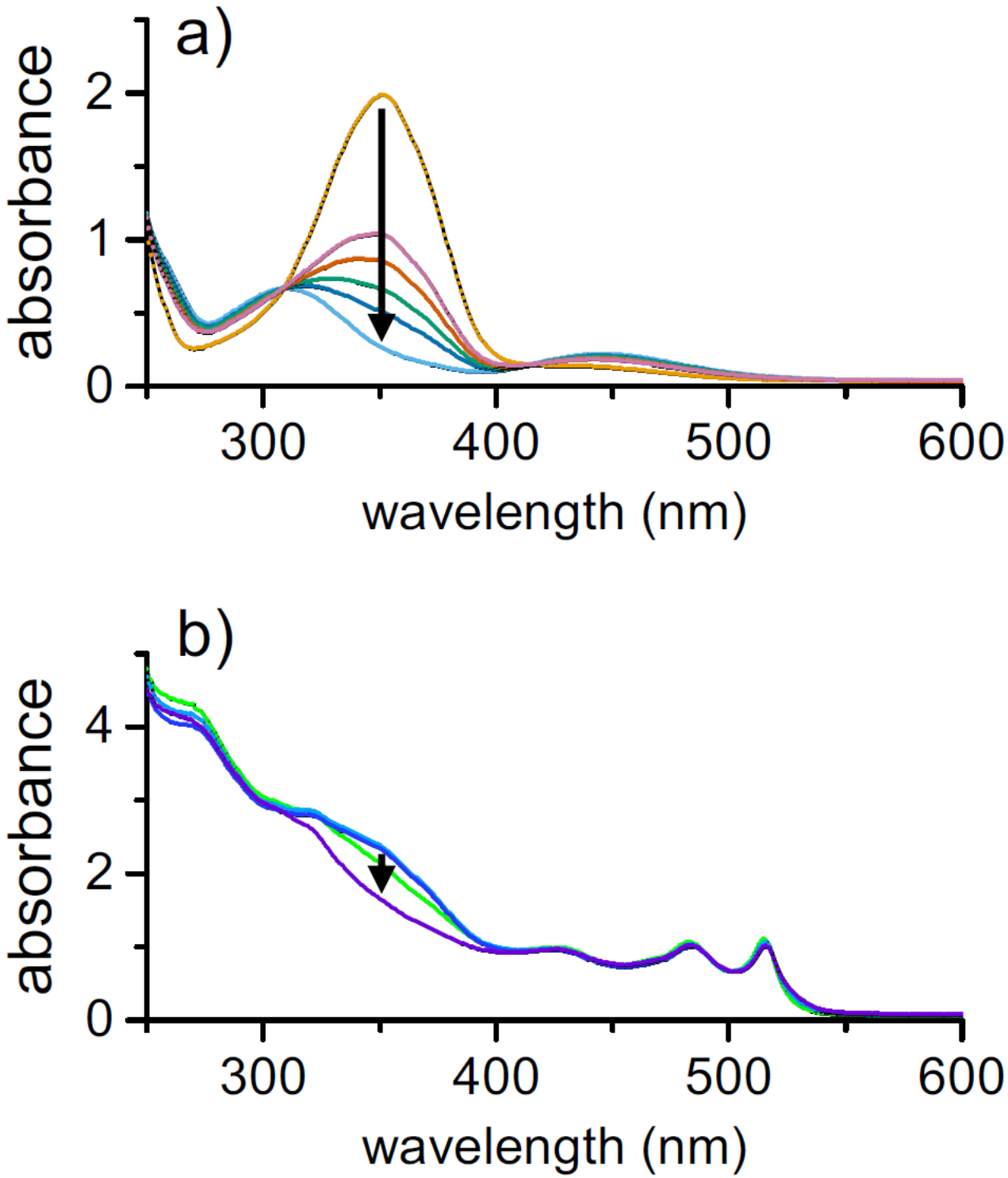


**Figure 4**

Monitoring azobenzene molecule (2) photo-switching under UV irradiation in solution and confined on nanoplatelets. a) UV visible spectra of a chloroform solution of (2) in the E-configuration (orange) and after 1 min irradiation at λ = 365 nm (light blue). Spectra from dark blue to purple where then recorded every minute upon thermal relaxation in the dark. b) UV visible spectra of a chloroform colloidal solution

of nanoplatelets decorated by (2): light blue: initial state; purple: after 1 min irradiation at λ = 365 nm; green: after 5 min thermal relaxation in the dark; dark blue: after 5 min relaxation under ambient light.

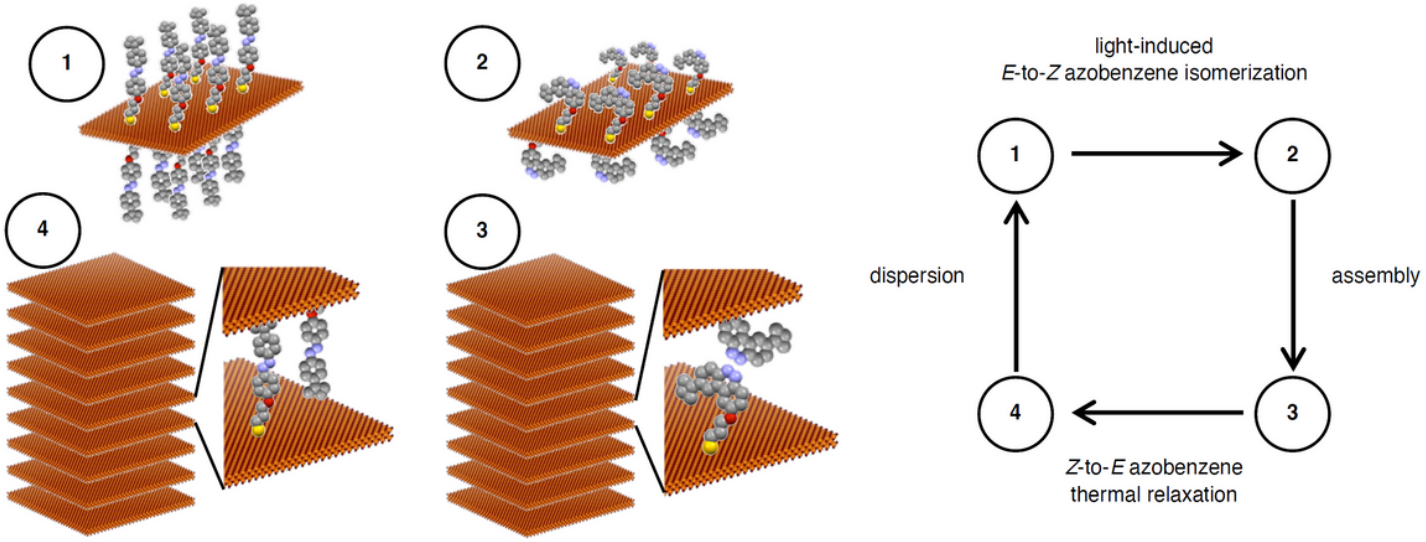


## Figure 5

Schematic representation of the assembly mechanism of CdSe nanoplatelets decorated by molecular photo-switch (2).

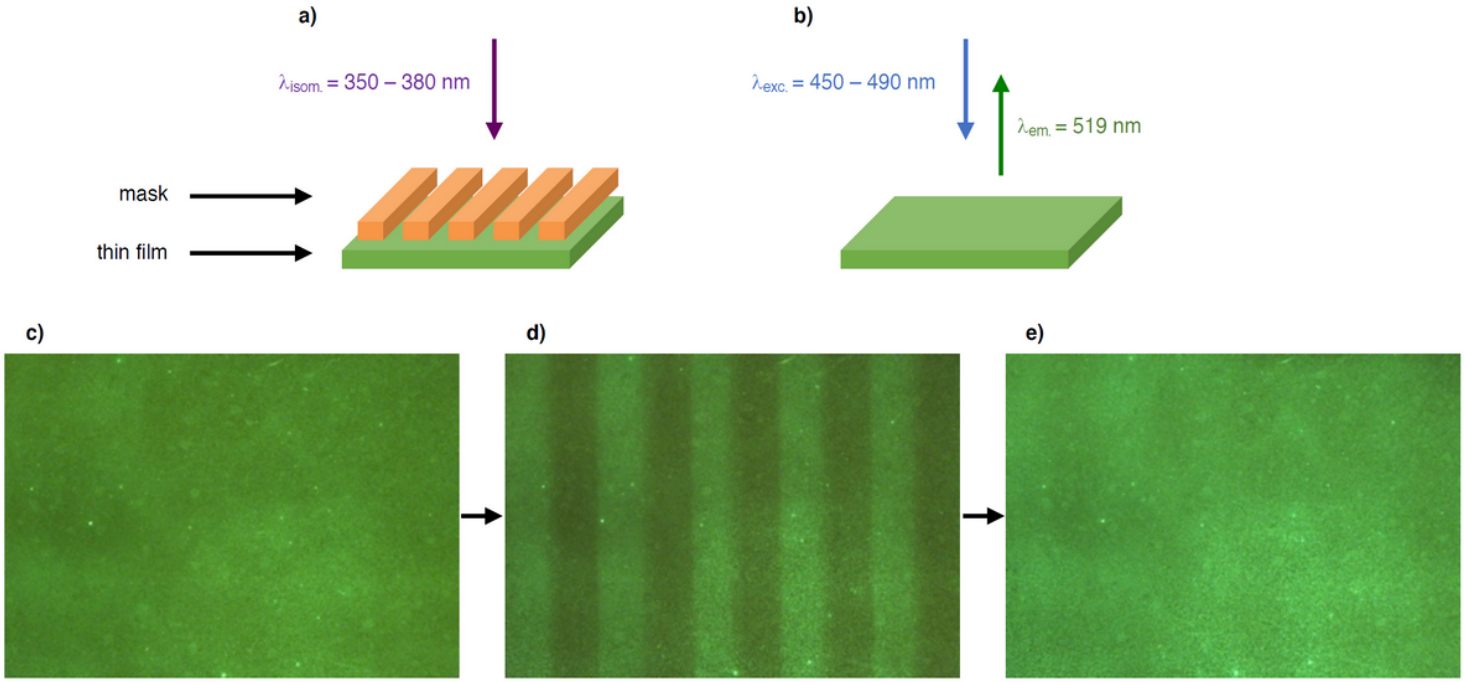


## Figure 6

Photo-patterning of thin films made of hybrid nanoplatelets using a fluorescence microscope and a mask. a) schematic representation of the experimental set-up used to pattern the sample under the microscope lens. The azobenzene isomerization is triggered in the range λisom. = 450 – 490 nm. b)

microscope settings to excite and read out the luminescence of the nanoplatelets before and after patterning. c) Homogenous green fluorescence of a thin film of nanoplatelets in solution, recorded before irradiation. The luminescence of the nanoplatelets was excited in the range λexc. = 450 – 490 nm. d) After irradiation at λisom. = 350 – 380 nm, the green fluorescence is enhanced in the irradiated areas, relatively to the masked areas, because the effective monomer concentration is decreasing in the irradiated areas, thus inducing a mass transfer from masked areas. e) Homogeneous fluorescence is recovered after 280 s.

## Supplementary Files

This is a list of supplementary files associated with this preprint. Click to download.

- SupplementaryInformation.pdf